

## Giant Optical Anisotropy of Semiconductor Heterostructures with No Common Atom and the Quantum-Confined Pockels Effect

Olivier Krebs and Paul Voisin

Laboratoire de Physique de la Matière Condensée de l'Ecole Normale Supérieure, 24 Rue Lhomond, F75005 Paris, France

(Received 30 January 1996)

We examine the optical anisotropy associated with the absence of fourfold rotoinversion axis in heterostructures of zinc-blend materials sharing no common atom or submitted to an external potential having no inversion symmetry. We discuss a simple original method allowing the introduction of the local symmetry considerations into the classical envelope function theory, which permits flexible calculations of quantum well structures. In particular, we consider the “quantum confined Pockels effect” resulting from the application of an external electric field, and we discuss its relation to the “quantum confined Stark effect.” [S0031-9007(96)00812-5]

PACS numbers: 73.20.Dx, 78.20.Jq, 78.66.-w

Semiconductor heterostructures in which the host materials  $M1$ ,  $M2$  do not share a common atom have the remarkable peculiarity that chemical bonds across the interfaces do not exist in either of the hosts. The general composition is  $M1-M2=C1A1-C2A2$ , where  $A$  and  $C$  stand for the anion and cation species. Interfaces are formed with  $A1C2$  and  $A2C1$  bonds, respectively. For instance, an InP-InGaAs-InP quantum well involves a virtual half monolayer of GaInP (InAs) at the first (second) interface. A now accepted consequence is that interface dipole contributions to the band offset differ at the  $M1-M2$  and  $M2-M1$  interfaces. Such band offset noncommutativity has been evidenced in the (InGa)As-InP [1] and InP-(AlIn)As [2] systems grown along the  $(0, 0, 1)$  axis, and shows fair agreement with theory [3]. A more subtle consequence, illustrated in Fig. 1, is the anisotropy associated with the fact that, at the  $M1-M2$  interface the  $C1A1$  bonds all lie in the  $(-1, 1, 0)$  plane while the  $A1C2$  bonds lie in the perpendicular  $(+1, 1, 0)$  plane. This anisotropy is not compensated at the other interface because the chemical bonds themselves are different. Hence, the growth axis  $z$  is not a fourfold rotoinversion axis anymore, which allows some polarization anisotropy for light propagating along  $z$ . In the language of group theory, heterostructures with one common atom belong to the  $D_{2d}$  point group, while those with no common atom belong to the lower symmetry  $C_{2v}$  group [4]. However, this obvious structural anisotropy does not lead to in-plane anisotropy of the electronic structure and optical properties within the standard envelope function theory [5] which, as a rule, neglects any effect occurring at the scale of a host lattice constant. Conversely, these polarization dependence effects should naturally appear in tight-binding calculations of the optical properties, since such calculations take into account the full symmetry properties [4,6]. Yet, to the best of our knowledge, optical anisotropy for zinc-blend heterostructures grown along  $(0,0,1)$  have not been thoroughly discussed in the literature, except for the small effects observed in the rather peculiar situation of GaAs-AlAs type II interfaces [7]. In contrast with the negative prediction

of the envelope function theory, it was recently observed that InP-AlInAs type II superlattices show a large linear dichroism and associated birefringence in the near-gap region [8], for light propagating along the growth direction. More generally, there should be a strong motivation for finding some way of including the local symmetry properties into the  $\mathbf{k}\cdot\mathbf{p}$  theory, which is known as an excellent first order approximation and allows flexible and convenient calculations of various quantum well configurations and their perturbation by external fields. The purpose of this Letter is to introduce an original method incorporating these effects in the envelope function theory. This heuristic model, generalized to the situation where an asymmetric external potential is added to the heterostructure potential, leads to the prediction of a novel “mesoscopic” optical nonlinearity with the  $X_{xyz}^{(2)}$  symmetry, the longitudinal “quantum confined Pockels effect.”

In the zinc-blend structure, each anion is surrounded by four cations, the corresponding chemical bonds being along the four  $(1,1,1)$ -type directions (see Fig. 1). Clearly, the classical crystal axis of the  $(0,0,1)$  type are not representative of the local arrangement of chemical bonds. For systems grown along the  $(0,0,1)$  axis, the  $M1-M2$  interface is the last  $A1$  plane of the  $M1$  layer, and the  $M2-M1$  interface the last  $A2$  plane of the  $M2$  layer. We define a monolayer  $C-A-C'$  as the anion plane and surrounding bonds on each side.

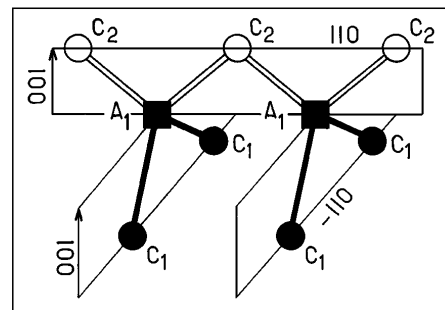


FIG. 1. Scheme of the chemical bond geometry in the zinc-blend crystals.

Choosing anion planes rather than cation planes as a reference is of course arbitrary, but physically consistent with the fact that epitaxy usually proceeds with anion-saturated surfaces. The general idea of our model is to attach to each monolayer operators  $P_j$  ( $j = 1, 4$ ) projecting the  $X$ ,  $Y$ , and  $Z$  orbitals onto the actual bond directions. We define  $|j\rangle = \frac{1}{2}| \pm (X + Y) + Z \rangle$ ,  $\frac{1}{2}| \pm (X - Y) - Z \rangle$ , and  $P_j = |j\rangle\langle j|$ . Pairing these four operators gives two operators  $B$  and  $F$  projecting on the “backward” and “forward” bonds.  $B$  and  $F$  matrix elements in the  $X, Y, Z$  basis are  $\langle i|B \text{ or } F|i\rangle = \frac{1}{2}$ ,  $\langle X \text{ or } Y|B|Z\rangle = \langle X \text{ or } Y|F|Z\rangle = 0$ ,  $\langle X|B|Y\rangle = -\frac{1}{2}$ , and  $\langle X|F|Y\rangle = \frac{1}{2}$ . As  $B + F = \text{identity}$ , the usual envelope-function valence band potential in an arbitrary system may be written as  $V_{\text{QW}}(z) + V_{\text{ext}}(z) = V(z) = \sum_{\ell} (B + F)V(z_{\ell})h(z - z_{\ell})$ , where  $h(z)$  is equal to 1 in the  $[-a/4, +a/4]$  segment and zero outside, and the summation runs over the anion plane positions  $z_{\ell}$ . This manipulation does not carry any physical meaning unless we consider a potential having no inversion symmetry (for instance electrostatical) or a valence band discontinuity corresponding to an interface. Indeed, in these cases, the Backward and Forward chemical bonds differ or experience different polarizations, which breaks the fourfold rotoinversion invariance around the  $z$  axis. In other words, the  $(1,1,0)$  and  $(-1,1,0)$  directions are no longer equivalent.

The induced anisotropy can be introduced in the theory by writing  $V(z) = \sum_{\ell} \{V(z_{\ell}) - (a/4)dV/dz\}h(z - z_{\ell})B + \{V(z_{\ell}) + (a/4)dV/dz\}h(z - z_{\ell})F$ . This amounts to associate to each *half* monolayer the corresponding average potential. Similarly, in the case of a compositional discontinuity involving a C1-A1-C2 monolayer, the valence band energy of the C1A1 material ( $V_1$ ) will be affected to the  $B$  operator and that of the C2A1 material ( $V_2$ ) to the  $F$  operator. These rules form a minimum model including the local symmetry effects and their necessary proportionality to the potential asymmetry. The sequence of C-A-C' monolayers in the presence of the external potential  $V_{\text{ext}}(z)$  is fully described by the succession of  $B$  and  $F$  operators with their associated potentials, as sketched in Fig. 2. It is clear that the classical envelope function description is recovered if one replaces the operators  $B$  and  $F$  by  $(B + F)/2 = \frac{1}{2}$ , and ignores the peculiarities of the interface chemical bonds. The differences between the present Hamiltonian  $H_{BF}$  and the envelope function Hamiltonian  $H_0$  are actually small and rapidly varying at the scale of the envelope functions. These are converging reasons for treating these differences in a perturbation scheme. More precisely, the perturbation  $\delta H = H_{BF} - H_0$  can conveniently be diagonalized in a truncated set of solutions of  $H_0$ . Reminding that the total wave function  $\Psi$  is the product of a slowly varying envelope function  $f(z)$  by a rapidly varying atomic-like Bloch function  $u(r)$  (more precisely, spinors built with such products) [4,5], it is clear that the

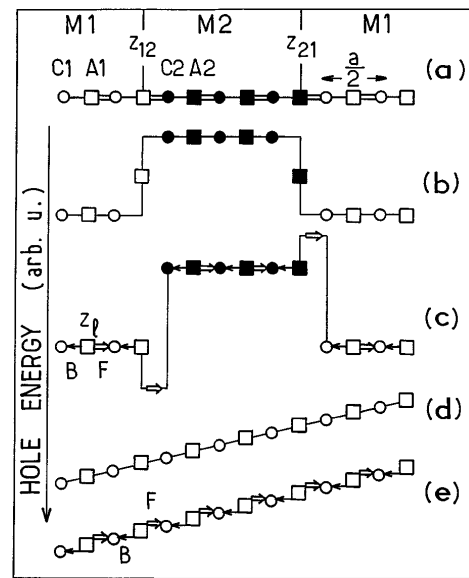


FIG. 2. The succession of cation and anion planes for a heterostructure grown along  $(0,0,1)$  (a), the associated envelope function potential (b), and the corresponding representation in terms of  $B$  and  $F$  operators (c). Bulk layer submitted to an electrostatical potential: envelope function potential (d) and its  $B$  and  $F$  operators representation (e).

rapidly varying perturbation will affect only the atomic part of the wave function, which contrasts with the traditional situation of slowly varying perturbation potentials affecting only the envelopes. In the following, for the sake of simplicity we restrict the algebra to the  $\Gamma_8$  basis, i.e., to the heavy- and light-hole states  $H_{\pm} = |3/2, \pm 3/2\rangle$  and  $L_{\pm} = |3/2, \pm 1/2\rangle$  [9]. Generalization to the full  $8 \times 8$   $\mathbf{k} \cdot \mathbf{p}$  Hamiltonian is straightforward. One easily checks that  $B$  and  $F$  have diagonal matrix elements all equal to  $\frac{1}{2}$  and in addition off-diagonal matrix elements  $\langle H+|F|L-\rangle = \langle H-|B|L+\rangle = i/2\sqrt{3}$  and  $\langle H-|F|L+\rangle = \langle H+|B|L-\rangle = -i/2\sqrt{3}$  which introduce a coupling between the heavy- and light-hole states. As discussed below, this results in a polarization anisotropy of the optical properties. The perturbation matrix element is  $M_{\mu,v}^{i,j} = \langle f_{\mu}^i | \delta H | f_{\nu}^j \rangle$ , where  $i$  ( $j$ ) is a subband index and  $\mu$  ( $\nu$ ) =  $H_{\pm}, L_{\pm}$ . In the spirit of the envelope function formalism, the envelope are slowly varying at the scale of  $a/2$ , which allows a factorization of the integrals. In the cases of a slowly varying potential  $V_{\text{ext}}(z)$  or a C1-A1-C2 interface, respectively, we straightforwardly get

$$M_{\mu,v}^{i,j} = \left\{ (a/4) \int f_{\mu}^i(z) f_{\nu}^j(z) \partial V_{\text{ext}} / \partial z dz \right\} \times \langle \mu | F - B | \nu \rangle, \quad (1)$$

$$M_{\mu,v}^{i,j} = (a/2) f_{\mu}^i(z_{12}) f_{\nu}^j(z_{12}) \times \{ [V_2' - (V_1 + V_2)/2] \langle \mu | F | \nu \rangle + [V_1 - (V_1 + V_2)/2] \langle \mu | B | \nu \rangle \}. \quad (2)$$

The perturbation matrix has diagonal elements producing small shifts of the valence band energy levels, which we shall ignore in the following. To illustrate the effects of the off-diagonal terms, i.e., the “mechanics” of the model, we restrict the basis to the  $H1\pm$  and  $L1\pm$  levels, and we describe the in-plane motion within the “diagonal” approximation where the in-plane dispersions are parabolic with masses [10]  $m_H^L$  and  $m_L^L$ . Although it is a crude approximation of the valence band structure, it has been proved that the diagonal model is quite sufficient to calculate accurately the band to band absorption spectrum [6,11]. In addition, valence subband mixing by the Luttinger matrix does not produce the optical anisotropy effects which we are looking for. The  $4 \times 4$  Hamiltonian matrix separates in two nearly identical  $2 \times 2$  matrices corresponding to the  $H1+$ ,  $L1-$  and  $H1-$ ,  $L1+$  subsets,

respectively. The first one is

$$\begin{pmatrix} H1 + h^2 k_x^2 / 2m_H^L & M_{H+L-} \\ M_{H+L-}^* & L1 + h^2 k_x^2 / 2m_L^L \end{pmatrix} \quad (3)$$

and the second one differs by the sign of the off-diagonal term,  $M_{H-L+} = -M_{H+L-}$ . We have chosen the “hole energy” notation with positive confinement energies and in-plane masses. The corresponding eigenfunctions are  $\Psi_{1,2} = a_{1,2} f_H |H+\rangle + b_{1,2} f_L |L-\rangle$ . Optical transitions to the first conduction subband induced by a photon propagating parallel to the  $z$  axis and polarized at an angle  $\theta$  with respect to the  $(1,0,0)$  axis can easily be calculated. As expected, the absorption spectrum  $A(h\nu, \theta)$  is polarization dependent. As  $M_{HL}$  (hence  $b_1$  and  $a_2$ ) are pure imaginary, we have, using the notations  $\underline{a}_i = a_i \langle f_E | f_H \rangle$ ,  $\underline{b}_i = b_i \langle f_E | f_L \rangle$ :

$$\begin{aligned} A/A_0 = & \{ \underline{a}_1^2 + \frac{1}{3} |\underline{b}_1|^2 - (2/\sqrt{3}) \underline{a}_1 |\underline{b}_1| \sin 2\theta \} Y(h\nu - (E_g + E1 + H'1)) \\ & + \{ |\underline{a}_2|^2 + \frac{1}{3} \underline{b}_2^2 + (2/\sqrt{3}) \underline{b}_2 |\underline{a}_2| \sin 2\theta \} (\mu_L^L / \mu_H^L) Y(h\nu - (E_g + E1 + L'1)), \end{aligned} \quad (4)$$

where  $Y(x)$  is the step function,  $A_0 \approx 6 \times 10^{-3} N_w$  is the absorption by the  $H1-E1$  transition calculated in the diagonal approximation, and  $N_w$  the number of quantum wells.  $\mu_{H(L)}^L$  is the in-plane reduced mass for the corresponding electron-hole pair, and  $H'1$  and  $L'1$  are the eigenenergies of Eq. (3). When deriving Eq. (4), we have assumed that  $|M_{HL}|$  remains small compared to the  $L'1-H'1$  energy separation in the energy range of interest. In these conditions, the polarization rate at the absorption edge is immediately obtained by the perturbation formula as  $P = (A_{\max} - A_{\min}) / (A_{\max} + A_{\min}) = (2/\sqrt{3}) (\langle f_E | f_L \rangle / \langle f_E | f_H \rangle) |M_{HL}| / (L1-H1)$ .

In practice, solutions of Eq. (3) for  $L1 - H1 = 32$  meV and  $|M_{HL}| = 0.74$  meV give the polarization spectra shown in Fig. 3. It is seen that a significant absorption anisotropy appears in the spectral range between the  $H1-E1$  and  $L1-E1$  transitions. In this energy range, the absorption is larger (or smaller, depending on the sign of  $M_{HL}$ ) for a photon polarization along  $(1,1,0)$  than for a polarization along  $(-1,1,0)$ . This linear dichroism also implies, via the Kramers-Kronig relations, a birefringence in the near band-gap region. Detailed comparison with experimental data is out of the scope of this Letter, but we note that these predictions are in close qualitative agreement with the observations reported recently by Seidel *et al.* for InP-(AlIn)As type II multiquantum wells [8], and may also explain the surprising result that blue-light vertical-cavity surface emitting lasers based on no common atom II-VI quantum wells are always strongly polarized along the  $(-1,1,0)$  direction [12]. More recently, these effects have been studied in InGaAs-InP type I quantum wells [13], and the results also show complete agreement with the present considerations. In particular, the width of the observed

polarization spectrum is clearly equal to the  $H1-L1$  splitting. As for the value of the polarization rate, the observed  $P = 11\%$  in a  $108 \text{ \AA}$  InGaAs-InP quantum well agrees with the present prediction if offset asymmetry and residual strain in the sample are taken into account, and an interface potential value of  $\approx 1$  eV is retained. This is an enormous effect, comparable with the optical anisotropy of quartz.

This model does not contain any fitting parameter and its quantitative comparison with experiments is a crucial test. In practice, however, the band offsets between the “virtual” interface materials  $C1A2$  and  $C2A1$  and the heterostructure hosts  $C1A1$  and  $C2A2$  are not known with sufficient accuracy, and the effect of an external electrostatic field would be an even better test. Evaluation of Eq. (1) with  $V(z) = eFz$  and the parameters of a GaAs-

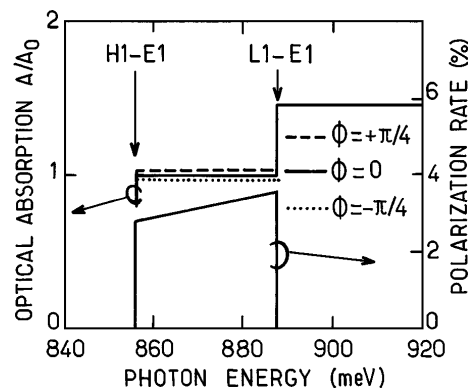


FIG. 3. Absorption spectra for various polarization angles  $\theta$  (a) and associated polarization spectrum (b). Calculations are for a supposedly symmetrical  $100 \text{ \AA}$  GaInAs-InP quantum well with  $M_{HL} = 0.74$  meV, which corresponds to  $(V_2' + V_1') - (V_1 + V_2) = 1$  eV.

AlGaAs 100 Å quantum well gives a polarization rate  $P = 4\%$  for  $F = 50$  kV/cm. Yet, the effect associated with Eq. (1) is only the polarization of chemical bonds in “bulk” of the host layers. The electric field has another effect which is the deformation of the classical envelope functions, known as the “quantum confined Stark effect.” This deformation affects moderately the overlap of the heavy- and light-hole envelopes appearing in Eq. (1), but changes drastically the respective weights of the  $M1$ - $M2$  and  $M2$ - $M1$  interface terms [Eq. (2)] which are directly sensitive to the values of the envelopes at the interfaces. In the regime where the energy shifts associated with the quantum confined Stark effect are quadratic, the latter effect is linear in  $F$ . In the case of common-atom quantum wells, the two interface contributions obviously cancel each other at  $F = 0$ , and should be revealed at  $F \neq 0$ . For instance, adding the two contributions gives a polarization rate  $P = 1.4\%$  for a 100 Å GaAs-Al<sub>0.3</sub>Ga<sub>0.7</sub>As quantum well under a 50 kV/cm electric field. Altogether, these effects and their consequences on the optical index in the transparency region form the quantum confined Pockels effect [14]. This is a large second order optical nonlinearity, specific to quantum well structures, and having the  $X_{xyz}^{(2)}$  symmetry. This effect contradicts the classical envelope function results [15] where such terms are forbidden.

In conclusion, we have introduced a simple theoretical model leading to a parameter-free prediction of optical anisotropies and optical nonlinearities in semiconductor heterostructures. Hole “spin” relaxation mechanisms [16,17] should also be considerably affected by the heavy- and light-hole mixing at  $k_x = 0$  in no common atom heterostructures. These are promising and stimulating results, supported by recent observations [8,12,13]. Yet, the present approach is essentially heuristic and must be confirmed by a comparison with a more complete theory. Tight-binding calculations should allow this *a posteriori* justification, as they can naturally take into account the local symmetry properties [4,18] on which our model is based. On a more technical ground, the influence of the actual valence subband dispersion, the contribution of upper-lying subbands, the role of Coulomb interaction, etc. must be evaluated. These complications cannot change the qualitative features, but may affect the quantitative results. Finally, detailed comparison with experimental results in various systems (for instance InGaAs-InP and InGaAs-AlInAs) must be undertaken in order to check the correctness and precision of the parametrical dependences on the quantum well thickness, band offsets, and applied electric field. Detailed observation of the quantum confined Pockels effect is an open challenge.

We thank Dr. R. Ferreira, Dr. W. Seidel, Dr. D. Bertho, and Dr. C. Jouanin for fruitful discussions. LPMC-

ENS is Unité de Recherche Associée au CNRS et aux Universités Paris VI et Paris VII. This work is supported in part by the IT OFCORSE program of the European Community.

- 
- [1] J.P. Landesman, J.C. Garcia, J. Massies, P. Maurel, G. Jezequel, J.P. Hirtz, and P. Alnot, *Appl. Phys. Lett.* **60**, 1241 (1992).
  - [2] E. Lugagne-Delpon, J.P. André, and P. Voisin, *Solid State Commun.* **86**, 1 (1991).
  - [3] Y. Foulon and C. Priester, *Phys. Rev. B* **45**, 6259 (1992). C. Priester, *J. Phys. III (France)* **1**, 481 (1991), and references therein.
  - [4] D.L. Smith and C. Mailhot, *Rev. Mod. Phys.* **62**, 173 (1990).
  - [5] G. Bastard, *Wave Mechanics Applied to Semiconductor Heterostructures* (Les Editions de Physique, les Ulis Cedex, France, 1988).
  - [6] Y.C. Chang and J.N. Schulman, *Phys. Rev. B* **31**, 2056 (1985); **31**, 2069 (1985).
  - [7] C. Gourdon and P. Lavallard, *Phys. Rev. B* **46**, 4644 (1992).
  - [8] W. Seidel, J.P. André, and P. Voisin, in *Proceedings of the 7th International Conference on Semiconductor Structures (MSSS7)*, Madrid, 1995 [*Solid State Electronics* (to be published)].
  - [9] We use  $H+ = (1/\sqrt{2})(X + iY) \uparrow$ ,  $H- = -(1/\sqrt{2})(X - iY) \downarrow$ ,  $L+ = (1/\sqrt{6})[(X + iY) \downarrow - 2Z \uparrow]$  and  $L- = -(1/\sqrt{6})[(X - iY) \uparrow + 2Z \downarrow]$ . Note that we are dealing with on-site atomiclike orbitals rather than true Bloch functions which are the sum of these orbitals over four equivalent intracell sites.
  - [10] If the effective mass differences between the hosts can be neglected, these in-plane masses are simply related to the confinement masses  $M_{H(L)}^Z$ . By  $m_H^i = 4m_H^z m_L^z / (3m_L^z + m_H^z)$  and  $m_L^i = 4m_H^z m_L^z / (3m_H^z + m_L^z)$ .
  - [11] S. Chelles, R. Ferreira, and P. Voisin, *Semicond. Sci. Technol.* **10**, 105 (1995).
  - [12] H. Jeon, V. Kozlov, P. Kelkar, A.V. Nurmikko, C.C. Chu, D.C. Grillo, J. Han, G.C. Hua, and R.L. Gunshor, *Appl. Phys. Lett.* **67**, 1668 (1995).
  - [13] W. Seidel, O. Krebs, J.P. André and P. Voisin (to be published).
  - [14] Field-induced anisotropy has already been observed in the emission by biased GaAs quantum wells. See S.H. Kwok, H.T. Grahn, K. Ploog, and R. Merlin, *Phys. Rev. Lett.* **69**, 973 (1992).
  - [15] J. Khurgin, *Phys. Rev. B* **38**, 4056 (1992).
  - [16] R. Ferreira and G. Bastard, *Phys. Rev. B* **43**, 9687 (1991).
  - [17] T. Uenoyama and L.J. Sham, *Phys. Rev. Lett.* **64**, 3070 (1990).
  - [18] D. Bertho and C. Jouanin (private communication).